Published in final edited form as:
J Phys Chem Lett. 2013 June 6; 4(11): 1924–1927. doi:10.1021/jz4008036.

Pump-Probe Microscopic Imaging of Jurassic-Aged Eumelanin

Mary Jane Simpson[1], **Keely E. Glass**[1], **Jesse W. Wilson**[1], **Philip R. Wilby**[2], **John D. Simon**[3], and **Warren S. Warren**[1]

Warren S. Warren: warren.warren@duke.edu

[1]Department of Chemistry, Duke University, Durham, NC 27705

[2]British Geological Survey, Keyworth, Nottingham NG12 5GG, United Kingdom

[3]Department of Chemistry, University of Virginia, Charlottesville, VA 22904

Abstract

Melanins are biological pigments found throughout the animal kingdom that have many diverse functions. Pump-probe imaging can differentiate the two kinds of melanins found in human skin, eumelanin and pheomelanin, the distributions of which are relevant to the diagnosis of melanoma. The long-term stability of the melanin pump-probe signal is central to using this technology to analyze melanin distributions in archived tissue samples to improve diagnostic procedures. This report shows that most of the pump-probe signal from eumelanin derived from a Jurassic cephalopod is essentially identical to that of eumelanin extracted from its modern counterpart, *Sepia officinalis*. However, additional classes of eumelanin signals found in the fossil reveal that the pump-probe signature is sensitive to iron content, which could be a valuable tool for pathologists who cannot otherwise know the microscopic distributions of iron in melanins.

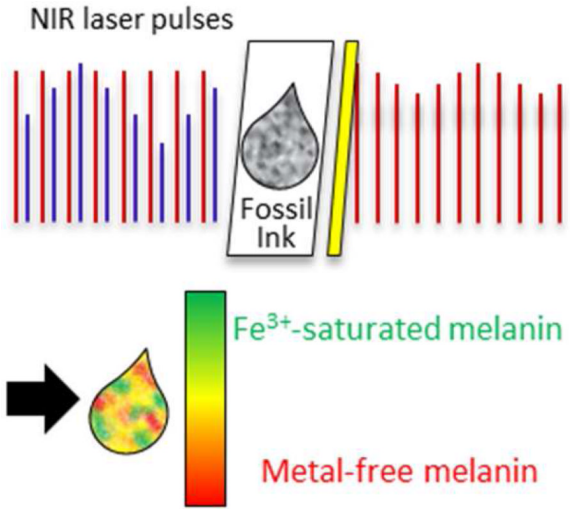

Keywords

eumelanin; nonlinear spectroscopy; melanoma; microscopy; iron; pigment

Paleontologists and pathologists alike are interested in melanin as a natural biomarker. In paleontology, it provides access to the coloring of ancient organisms (1). Direct chemical

Correspondence to: Warren S. Warren, warren.warren@duke.edu.

analysis has confirmed the similarity between eumelanins from Jurassic and modern cephalopods, showing that eumelanin can resist degradation for over 160 million years (2), much longer than many biomolecules. In pathology, the types and distributions of melanin are relevant to the diagnosis of melanoma (3). Pump-probe microscopy identifies the types of melanin and their relative distributions in tissue based on transient absorption measurements with nearinfrared laser pulses (3). Because melanin is poorly understood, chemical analysis of the Jurassic eumelanin does not guarantee that the feature giving rise to the pump-probe response is preserved for millions of years; however, imaging Jurassic eumelanin demonstrates the long-term stability of the pump-probe eumelanin signature. This potentially permits imaging of archived tissue samples in retrospective databases to improve diagnostic procedures—an approach that is usually not possible with more traditional immunohistochemical methods (4).

In this letter, we show that the pump-probe signature of most of the eumelanin from the ink sac of a Jurassic cephalopod (GSM 122841) is identical to that of its modern counterpart, validating its stability as a biomarker for analyzing archived pigmented tissue. However, we also find variations in the fossilized specimen, which can be reproduced in modern specimens by changing the iron content. Although not considered in earlier work, this is potentially valuable information for pathologists because iron levels are increased in metastatic melanoma (5).

Pump-probe microscopy is an emerging molecular imaging technique based on temporal responses to optical excitation. The pump-probe signal reflects a variety of time-dependent competing multi-photon processes, such as excited state absorption and ground state depletion, stimulated Raman, and the excited state lifetime (6), and thus can produce a highly structured molecular signature by varying the optical delay. This allows differentiation of molecules that have similar absorption spectra, as in UV-Vis spectroscopy. We vary the optical delay between pump and probe pulses (720 nm and 810 nm, respectively) and monitor the transmitted probe intensity via a modulation transfer technique, producing a set of images. By convention, a positive signal indicates an increase in probe absorption, while a negative signal indicates either a decrease in absorption or stimulated emission.

Pump-probe imaging of the unpurified contents of the fossil ink sac revealed a molecular signature resembling purified eumelanin from the ink sac of modern *Sepia officinalis*; this signature was not present in the fossil background sediment. The averaged pump-probe response of selected regions of melanin-like pixels in the fossil is shown as the solid, cyan line in Figure 1; the response of the purified modern eumelanin is shown as the dashed, magenta line. The signal is negative when the pump and probe pulses are overlapped in time (at $t = 0$) and is most likely a ground state bleach (6). It is followed by a positive signal when the pump precedes the probe ($t > 0$), an excited-state absorption signal.

The fossil ink also contained particles that do not match the response of the modern, purified eumelanin. Phasor analysis, which identifies pixels with similar types of behavior using no *a priori* knowledge (7), was used to identify particles that do not match the purified eumelanin pump-probe response. The phasor plot of the fossil eumelanin is shown in Figure 2a. The plot is a histogram of all the pixels in the pump-probe image (Figure 2c), and pixels that behave similarly cluster together and are colored based on their clusters. The behavior of pixels in a cluster are averaged together to represent the average response giving rise to the signals.

The data are clustered about two extremes, region 1, circled in red and region 2, circled in dashed green. Pixels in the pump-probe images with behavior similar to the positive signal,

characterizing region 1, are false-colored red; and those with the negative signal, characterizing region 2, are false-colored green; and intermediate behavior is colored according to an interpolated path shown in Figure 2a. The average eumelanin signals in Figure 1 are linear combinations of the response from regions 1 and 2. Eumelanin from *S. officinalis* is most similar to region 1, with very little contribution from region 2, so it is colored red-orange in the corresponding pump-probe image (Figure 2c).

To determine the source of pixels in region 2, which are not present in the modern purified eumelanin (Figure 2d), we considered molecular components that naturally occur in unpurified modern ink, as well as organic and inorganic species associated with fossil inks (2). Apatite, a diagenetic mineral associated with the fossil ink in relatively high concentrations (2), failed to give any pump-probe signal. The responsible material must have an electronic excited state with sufficiently low energy to allow a visible/near-infrared absorption, which is rare in organic molecules (and requires conjugation), but is common in transition metal complexes with available d-orbitals (8). Eumelanin from *S. officinalis* is normally bound to a variety of transition metals such as manganese, iron, copper, cobalt, palladium, and nickel (9), and these metals are so persistent that they can be used as a biomarker for the presence of eumelanin even in fossils (10).

Washing melanins with EDTA can remove the majority of bound metals (9). Figure 3 compares the pump-probe signature of pure eumelanin from *S. officinalis* before and after washing. The EDTA-washed eumelanin has a response similar to the red pixels in Figure 2b with no green-colored pixels contributing to the signal. This suggests that bound metals are the source of pixels in region 2 and metal-free eumelanin is the source of those in region 1. Direct confirmation of the difference in metal content between the fossil and modern *S. officinalis* eumelanin was not possible, as it would require the destruction of the fossil sample.

In order to confirm the impact of bound metals on the pump-probe behavior of eumelanin, we imaged eumelanin loaded with iron and copper. Iron(III) and copper(II) were chosen because they are transition metals with available d-orbitals and are present in natural melanin (9). Eumelanin previously washed with EDTA was loaded with iron(III) chloride or copper(II) chloride (9). Eumelanin loaded with copper(II) chloride had a signature identical to that of EDTA-washed eumelanin. However, iron-loaded eumelanin showed a response similar to the green pixels in region 2 of the fossil ink. In the same color scheme as before, Figure 4 shows that eumelanin washed with EDTA is the source of the red pixels in region 1, and eumelanin loaded with iron is the source of the green pixels in region 2. The yellow/orange pixels in between these two extremes have intermediate levels of metal content. As shown by the phasor analyses, few pixels in the fossil image are clustered where the EDTA-washed eumelanin pixels are clustered. Therefore, we conclude that most of the fossil pigment contains at least some bound metal, however the amount varies widely across the field of view.

The linear combination of the iron-free eumelanin and the iron-loaded eumelanin could allow an approximation of the iron content based on the shape of the pump-probe signature. Figure 5 shows the pump-probe response of EDTA-washed *S. officinalis* eumelanin loaded with different initial concentrations of iron(III) chloride. The eumelanin is saturated with iron when the initial concentration of iron is greater than 1 μM (9). Increasing the initial iron concentration causes the negative signal when the pulses are overlapped (at $t = 0$) to appear and the positive signal when the pump precedes the probe ($t > 0$) to disappear; the 0.25 μM is similar to the *S. officinalis* eumelanin response given in Figure 1. This value is approximately in agreement with the reported concentrations found in natural *S. officinalis* melanin (9).

This letter has shown that eumelanin preserved in the fossilized ink sac of a Jurassic cephalopod (GSM 122841) has a similar pump-probe signature as its modern counterpart in *S. officinalis*. Comparing the signature of metal-free and iron-loaded eumelanin suggests the pumpprobe signal changes are associated with metal-binding. This reveals that the unpurified fossil contains a wide range of iron levels, whereas modern, purified *S. officinalis* eumelanin is mostly iron-free.

In conclusion, the shape of the eumelanin pump-probe delay curve allows for the imaging of the microscopic distribution and concentration of melanin-bound iron. In biopsies of pigmented human tissue, phasor analysis gives a wide range of pump-probe responses, and this work shows that some of that response might be due to metal ion binding by the melanin, potentially providing additional options for molecular specificity to pathologists.

Experimental

Imaging was done with a two-color pump-probe microscope as described previously (3). The samples were imaged dry on a glass slide with a 0.75 NA, 40× objective with approximately 0.2 mW average power in each beam.

Phasor analysis software, written in Matlab and identical to that previously reported (7), was used to analyze the curves to find clusters of pixels with similar pump-probe behavior. Regions of interest were selected based on these clusters, and the image was false-colored based on the pixels contained in the regions of interest.

Melanin used in this experiment was Sigma-Aldrich *S. officinalis* melanin powder that had been previously prepared and analyzed (9). Methods for washing with EDTA and loading with iron(III) chloride and copper(II) chloride have previously been reported (9).

Fossil specimen GSM 122841, an approximately 162 million years old cephalopod ink sac, was collected from the Peterborough Member of the Oxford Clay Formation (middle Jurassic, Upper Callovian) at Christian Malford, Wiltshire (UK) and is currently held in the collections at BGS, Keyworth. Portions of the ink and the sediment surrounding the ink sac were removed by etching the specimen with the tip of a screwdriver. These portions were then separately ground to fine powders with a mortar and pestle.

Acknowledgments

We gratefully acknowledge NIH grant R01-CA166555 (WSW) and NIH fellowship no. 1F32CA168497-01A1 (JWW).

References

1. McNamara ME. The Taphonomy of Colour in Fossil Insects and Feathers. J. Paleo. 2013; 3:557–575.
2. Glass KE, Ito S, Wilby PR, Sota T, Nakamura A, Bowers CR, Vinther J, Dutta S, Summons R, Briggs DEG, et al. Direct Chemical Evidence for Eumelanin Pigment from the Jurassic Period. Proc. Natl. Acad. Sci. U.S. A. 2012; 109:10218–10223. [PubMed: 22615359]
3. Matthews TE, Piletic IR, Selim MA, Simpson MJ, Warren WS. Pump-Probe Imaging Differentiates Melanoma from Melanocytic Nevi. Sci. Transl. Med. 2011; 3:71ra15.
4. Xie R, Chung JY, Ylaya K, Williams RL, Guerrero N, Nakatsuka N, Badie C, Hewitt SM. Factors Influencing the Degradation of Archival Formalin-Fixed Paraffin-Embedded Tissue Sections. J. Histochem. Cytochem. 2011; 59:356–365. [PubMed: 21411807]
5. Baldi A, Lombardi D, Russo P, Palescandolo E, De Luca A, Santini D, Baldi F, Rossiello L, Dell'Anna ML, Mastrofrancesco A, et al. Ferritin Contributes to Melanoma Progression by

Modulating Cell Growth and Sensitivity to Oxidative Stress. Clin. Cancer Res. 2005; 11:3175–3183. [PubMed: 15867210]

6. Ye T, Fu D, Warren WS. Nonlinear Absorption Microscopy. Photochem. Photobiol. 2009; 85:631–645. [PubMed: 19170931]
7. Robles FE, Wilson JW, Fischer MC, Warren WS. Phasor Analysis for Nonlinear Pump-Probe Microscopy. Opt. Exp. 2012; 20:17082–17092.
8. Rodgers, GE. Introduction to Coordination, Solid State, and Descriptive Inorganic Chemistry. New York, NY, U.S.A: McGraw-Hill; 1994.
9. Wogelius RA, Manning PL, Barden HE, Edwards NP, Webb SM, Sellers WI, Taylor KG, Larson PL, Dodson P, You H, et al. Trace Metals as Biomarkers for Eumelanin Pigment in the Fossil Record. Science. 2011; 333:1622–1626. [PubMed: 21719643]
10. Liu Y, Hong L, Kempf VR, Wakamatsu K, Ito S, Simon JD. Ion-Exchange and Adsorption of Fe (III) by Sepia Melanin. Pig. Cell Res. 2004; 17:262–269.

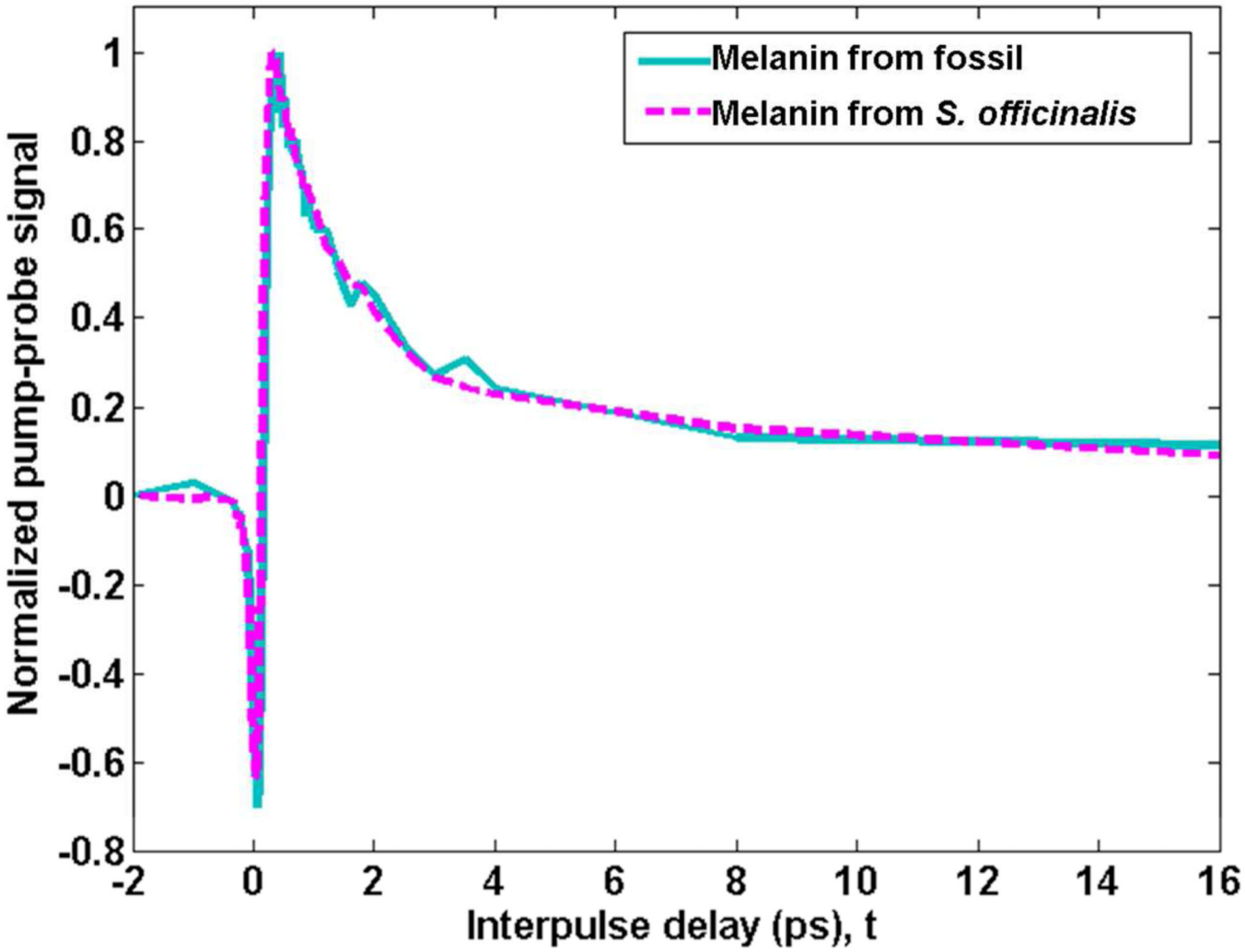

Figure 1.
Average pump-probe response of unpurified eumelanin from the fossil compared to purified eumelanin from *S. officinalis*. Signals are normalized to the positive peak for comparison.

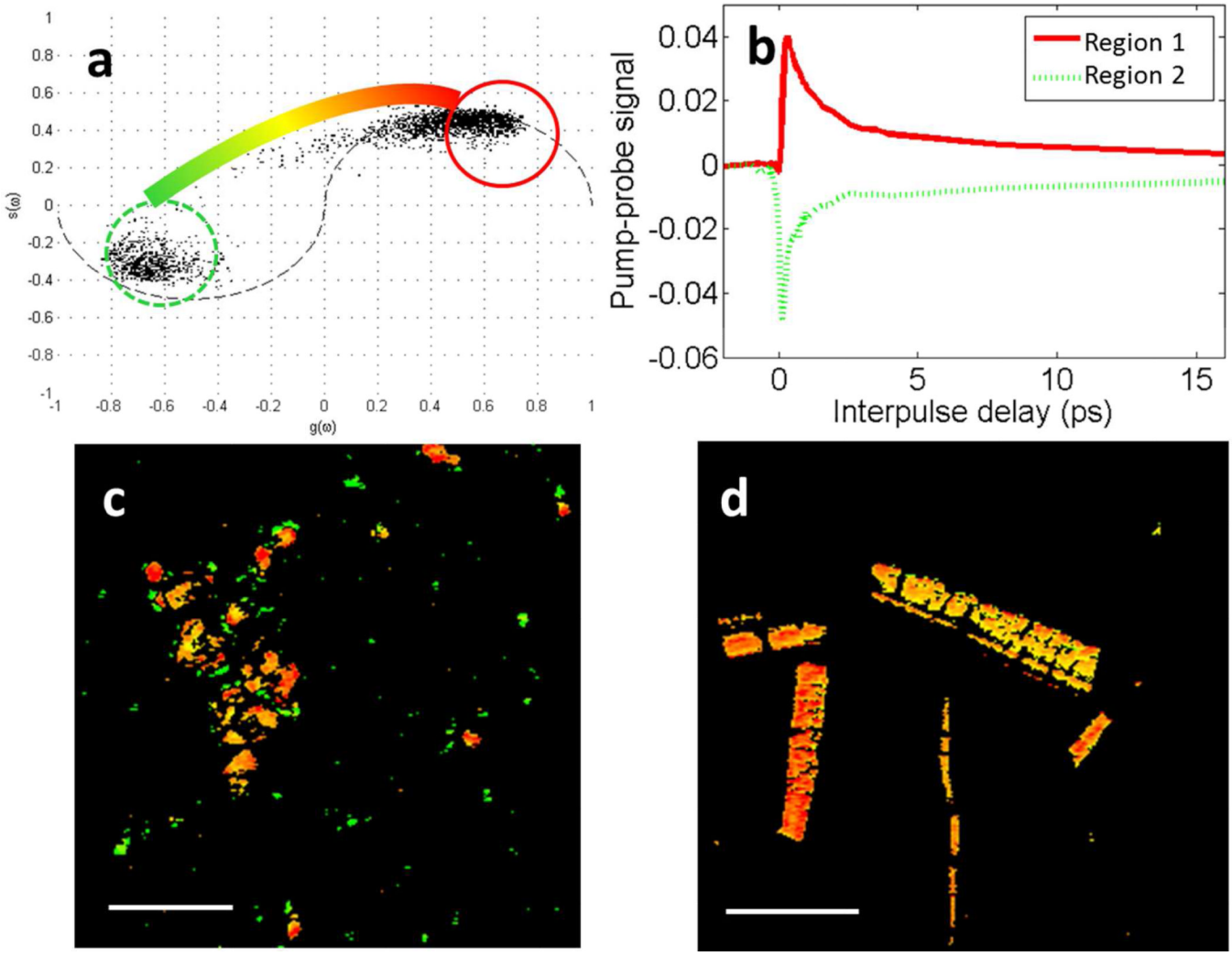

Figure 2.

a.) Phasor plot showing clusters of pixels with similar response in the unpurified fossil eumelanin. The color bar shows the color scheme used for pump-probe images, where pixels falling into the circles are colored accordingly, and pixels between those circles are interpolated to a shade in between. b.) Averaged pixels in corresponding regions of the phasor plot. c.) Pump-probe image of the fossil eumelanin on a glass slide with pixels colored according to the phasor color scheme. Scale bar = 100 μm. d.) Pump-probe image of purified *S. officinalis* eumelanin on a glass slide with pixels colored according to the phasor color scheme. Scale bar = 100 μm.

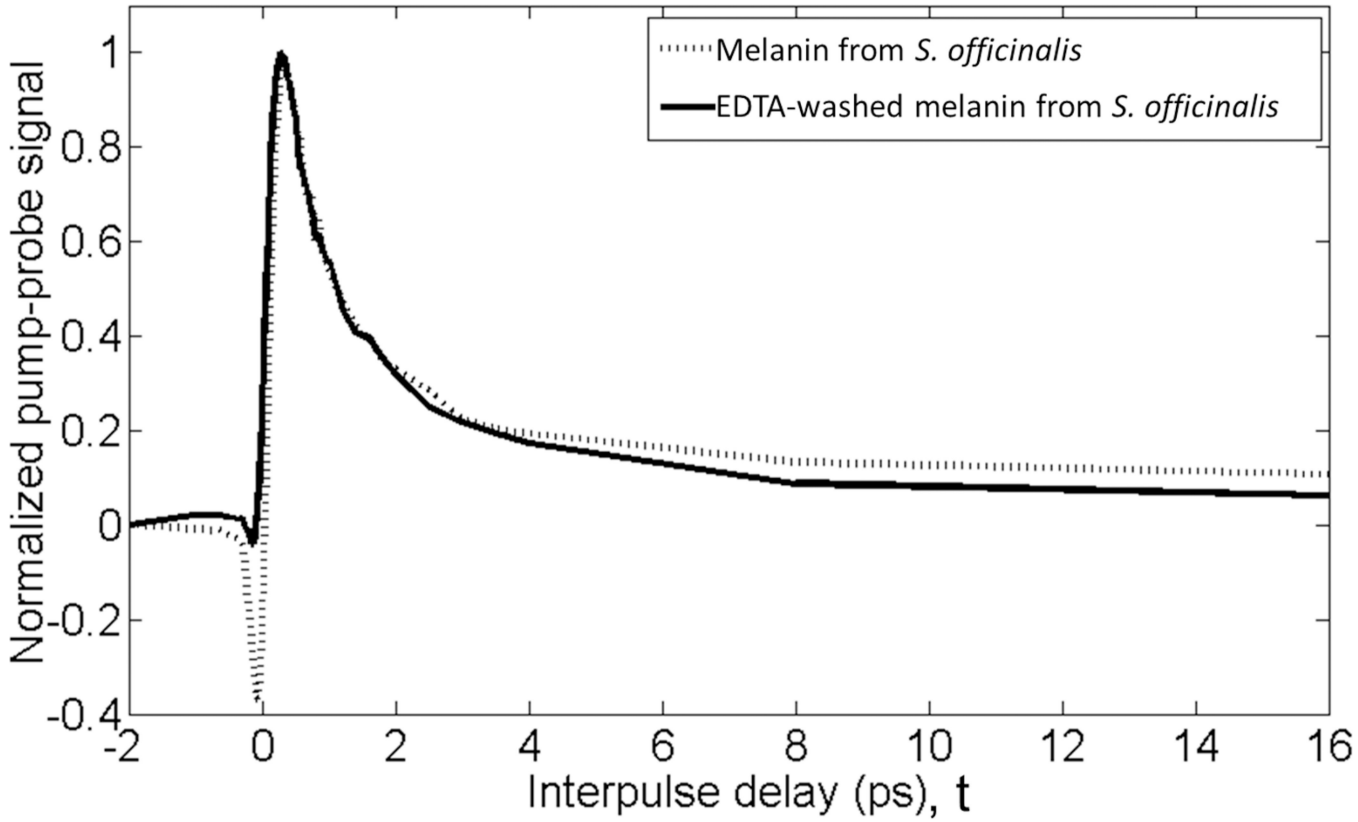

Figure 3.
Average pump-probe response of *S. officinalis* eumelanin washed with EDTA and unwashed. Traces are averaged from images in figures 2d and 4c.

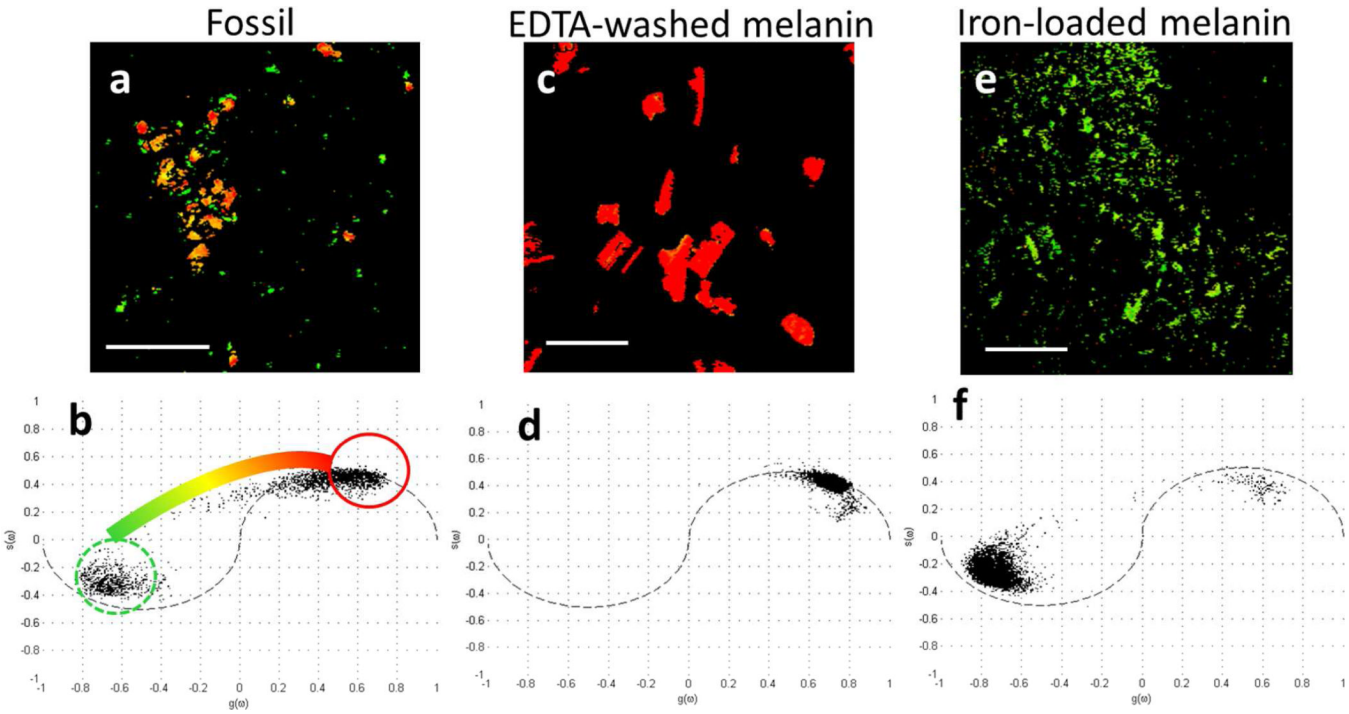

Figure 4.

a.) Pump-probe image of the fossil eumelanin with phasor color scheme. Scale bar is 100 μm. b.) Phasor plot of pixels in the imaged fossil, showing the color scheme used for the images. c.) Pump-probe image of *S. officinalis* eumelanin washed with EDTA. Scale bar is 100 μm. d.) Phasor plot of pixels in the imaged EDTA-washed *S. officinalis* eumelanin. e.) Pump-probe image of *S. officinalis* eumelanin washed with EDTA, then loaded with iron(III) chloride. Scale bar is 100 μm. f.) Phasor plot of pixels in the imaged iron loaded EDTA-washed S. *officinalis* eumelanin.

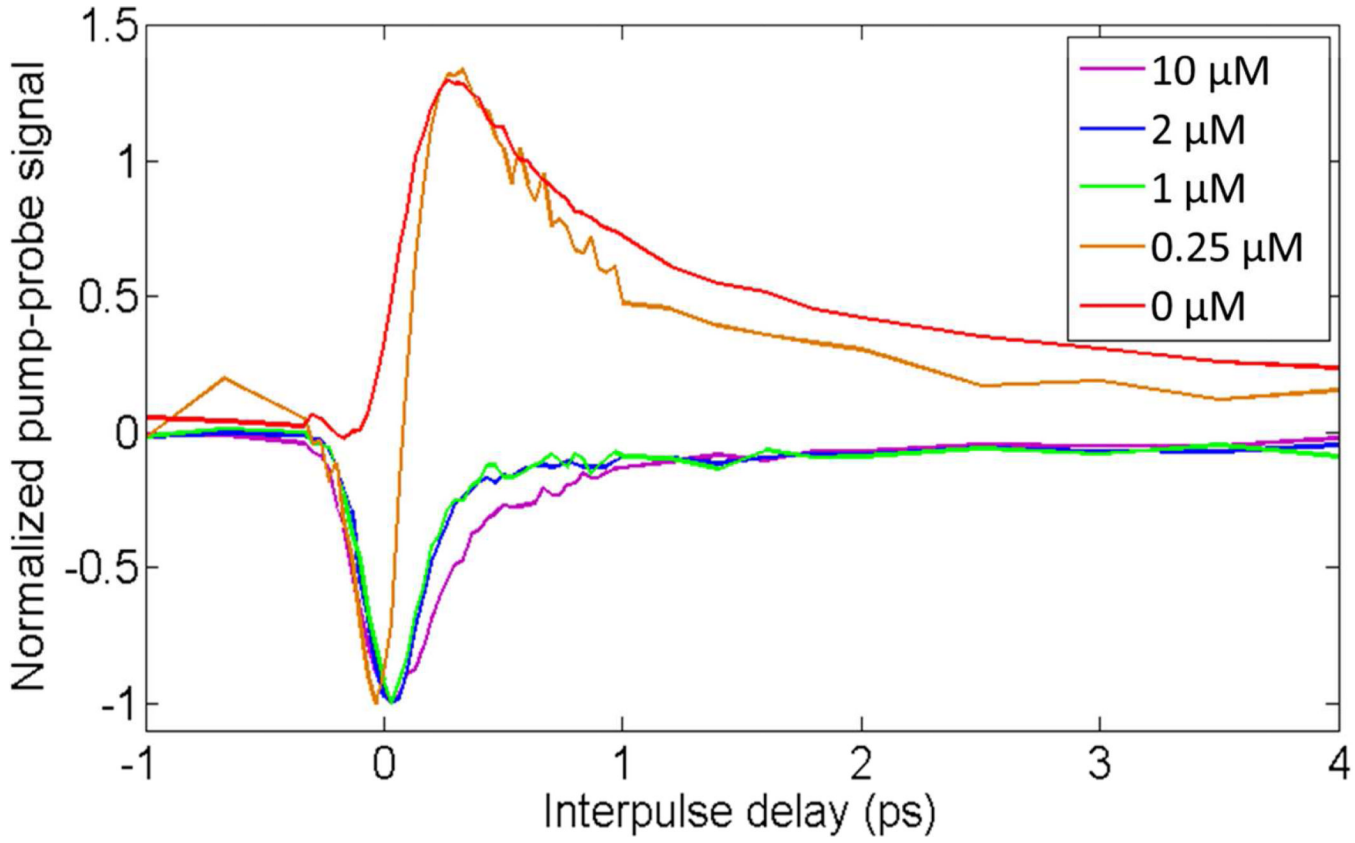

Figure 5.
Average pump-probe responses of iron-loaded *S. officinalis* eumelanin obtained by varying the initial concentration of iron(III) chloride.